THE JOURNAL OF PHYSICAL CHEMISTRY B
A JOURNAL OF THE AMERICAN CHEMICAL SOCIETY

pubs.acs.org/JPCB
Article

Simulating the Competitive Ion Pairing of Hydrated Electrons with Chaotropic Cations

Hannah Y. Liu, Kenneth J. Mei, William R. Borrelli, and Benjamin J. Schwartz*

Cite This: J. Phys. Chem. B 2024, 128, 8557−8566
Read Online

ACCESS | Metrics & More | Article Recommendations | Supporting Information

ABSTRACT: Experiments show that the absorption spectrum of the hydrated electron (e^-_{hyd}) blue-shifts in electrolyte solutions compared with what is seen in pure water. This shift has been assigned to the e^-_{hyd}'s competitive ion-pairing interactions with the salt cation relative to the salt anion based on the ions' positions on the Hofmeister series. Remarkably, little work has been done investigating the e^-_{hyd}'s behavior when the salts have chaotropic cations, which should greatly change the ion-pairing interactions given that the e^-_{hyd} is a champion chaotrope. In this work, we remedy this by using mixed quantum/classical simulations to analyze the behavior of two different models of the e^-_{hyd} in aqueous RbF and RbI electrolyte solutions as a function of salt concentration. We find that the magnitude of the salt-induced spectral blue-shift is determined by a combination of the number of chaotropic Rb^+ cations near the e^-_{hyd} and the number of salt anions near those cations so that the spectrum of the e^-_{hyd} directly reflects its local environment. We also find that the use of a soft-cavity e^-_{hyd} model predicts stronger competitive interactions with Rb^+ relative to I^- than a more traditional hard cavity model, leading to different predicted spectral shifts that should provide a way to distinguish between the two models experimentally. Our simulations predict that at the same concentration, salts with chaotropic cations should produce larger spectral blue-shifts than salts with kosmotropic cations. We also found that at high salt concentrations with chaotropic cations, the predicted blue-shift is greater when the salt anion is kosmotropic instead of chaotropic. Our goal is for this work to inspire experimentalists to make such measurements, which will help provide a spectroscopic means to distinguish between simulations models that predict different hydration structures for the e^-_{hyd}.

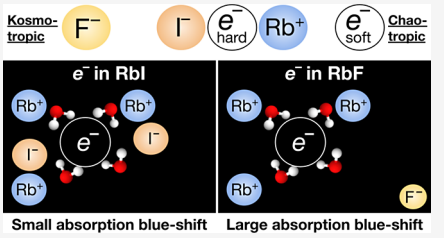

INTRODUCTION

The hydrated electron (e^-_{hyd}) is an excess electron that is solvated by liquid water.[1] Despite a huge amount of interest in hydrated electrons, their structure (e.g., the nature of any cavities in which they reside, the way the first-shell water molecules are arranged around the center of charge density, and so forth) is not known experimentally.[2−8] This means that most of what we know about e^-_{hyd} structure comes from computer simulations. Different simulations, however, use different levels of theory (e.g., mixed quantum/classical (MQC),[9−12] density functional theory (DFT),[13−16] and so forth[17]), and different levels of theory predict different structures. Most theoretical studies of hydrated electrons have focused on their behavior in pure water,[18] but e^-_{hyd}'s are also important in radiation chemistry and other chemical environments where there is a high concentration of salt. Thus, in this work, we continue our simulation-based investigation of the properties of e^-_{hyd}'s in electrolyte solutions.[19−24] What we find is that the way that hydrated electrons interact with different salts depends sensitively on the simulated e^-_{hyd}'s structure so that experiments on hydrated electrons in electrolyte solutions can infer a great deal about the e^-_{hyd}'s solvation environment.

Experimentally, it is known that the addition of salt leads to a modest blue-shift of the hydrated electron's absorption spectrum without any noticeable change in shape.[25−28] This observation is quite different from what happens to solvated electrons in other solvents, where excess electrons are known to form tight-contact pairs (TCPs) with salt cations. Such contact pairs have an absorption spectrum that lies midway between that of a pure solvated electron and the fully reduced cation species.[29−33] The fact that the salt-induced spectral shift is modest in water argues that aqueous electrons do not form TCPs with most salt species, preferring to remain independently solvated even in high-concentration aqueous salt solutions. Simulations indeed show that solvated electrons in aqueous electrolytes do largely retain their identity, but the precise nature of cation:electron pairing depends quite sensitively on the level of theory,[22] particularly the simulated interaction between the water and the cation.[21]

The salt-induced spectral blue-shift of the e^-_{hyd} is known experimentally to start quickly and then saturate with increasing salt concentration.[26] It is also experimentally known that multivalent cations yield larger spectral shifts

Received: June 27, 2024
Revised: August 10, 2024
Accepted: August 13, 2024
Published: August 23, 2024

https://doi.org/10.1021/acs.jpcb.4c04290
J. Phys. Chem. B 2024, 128, 8557−8566

than monovalent cations at the same salt concentration.[26] We simulated these effects with MQC molecular dynamics (MD) simulations and found that the concentration-dependent shift results from an increase in the number of cations in the proximity of the electron with increasing salt concentration, where association of the second and third cations causes much less spectral shift than the first.[20] Our simulations also suggested that multivalent cations cause larger spectral shifts because more of them associate with hydrated electrons than monovalent cations at the same concentration.[19] However, MQC simulations predict a salt-induced spectral blue-shift that is an order of magnitude larger than that seen experimentally as well as a spectral shape change.[19,21,36] This suggests that the MQC-simulated interaction between the e^-_{hyd} and cations is too strong.[20] Ab initio simulations based on DFT also have explored cation:e^-_{hyd} pairing, but they predict a spectral shift that is not only too large but also goes in the wrong direction.[22]

One interesting feature of the behavior of hydrated electrons in salt solutions is that the observed spectral shift depends not only on the identity of the electrolyte cation but also the anion; for example, perchlorate salts generally produce larger e^-_{hyd} spectral shifts than chloride salts with the same cation.[26] We argued based on MQC simulations that this results from the fact that many salts form strong cation:anion pairs in aqueous solution, and that when an anion is strongly paired with a cation, it decreases the strength of cation:e^-_{hyd} interaction, thus reducing the extent of the blue-shift of the hydrated electron's absorption spectrum.[19] This observation suggests that one can infer information about the solvation structure of the e^-_{hyd} by examining its competitive ion pairing with different salts: the idea is to see whether the hydrated electron is more or less likely to pair with a cation than a given anion, thus bracketing the possible solvation structures of the e^-_{hyd} as being more or less similar than those of various anions.

The main hypothesis to be tested via MQC MD simulation in this paper is that the competitive ion pairing of hydrated electrons with different salts is determined by their positions on the Hofmeister series,[37] i.e., by the details of how each cation and anion is solvated by water. Small salt ions with high charge density are referred to as kosmotropes, or structure makers; the first-shell waters are usually strongly oriented around such ions, leading to strongly negative solvation entropies.[38−40] On the other hand, larger salt ions with lower charge density are referred to as chaotropes, or structure breakers; these ions are hydrophobically solvated, with water preferring to make H-bonds around the ion, leading to weakly negative or positive solvation entropies.[39,40] In general, kosmotropic and chaotropic ions prefer to pair more strongly with other kosmotropes and chaotropes, respectively, so that only mixed kosmotrope/chaotrope salts typically have the ions fully solvated independently.[41] Since hydrated electrons are champion chaotropes with a highly positive solvation entropy,[39,40] one would expect them to pair more strongly with more chaotropic cations, such as Rb^+, than kosmotropic cations such as Na^+ or Ca^{2+}. To date, however, only a limited portion of the experimental work on e^-_{hyd}'s in electrolytes and none of the simulation work have explored the behavior of hydrated electrons in the presence of salts with chaotropic cations.

Thus, in this work, we extend our previous MQC simulation studies of hydrated electrons in electrolyte solutions in two new ways. First, we analyze how e^-_{hyd}'s behave in systems with a mildly chaotropic cation, exploring their interactions with both RbF (kosmotropic anion) and RbI (chaotropic anion) as a function of salt concentration. Second, we also examine the pairing behavior using two different e^-_{hyd} pseudopotentials: the Turi-Borgis (TB) potential,[42] which produces a fairly hard cavity and which we used in our previous work,[19−23,43] and a modified version of the TB pseudopotential with optimized polarization (TB-Opt),[11,22] which produces a much softer cavity structure than the original TB potential. We note that the TB-Opt potential is very similar to a recently developed potential that was empirically optimized to reproduce the e^-_{hyd}'s experimental vertical detachment energy and radius of gyration.[44] Based on the difference in the softness of their cavities, we would expect the TB-Opt hydrated electron to be more chaotropic than the TB hydrated electron.

Despite the expected difference in how chaotropic the two hydrated electron models are, we find that for both of them, the electron is more strongly associated with Rb^+ ions in RbF than RbI. This result makes sense since RbF is a mixed chaotrope/kosmotrope salt that has little cation:anion pairing, leaving Rb^+ in RbF free to pair with the e^-_{hyd}. However, unlike what we saw with Na^+ and Ca^{2+},[19] neither hydrated electron model forms direct contact pairs with Rb^+; instead, both e^-_{hyd} models prefer to form solvent-separated pairs wherein the cations are separated from the hydrated electron by roughly one water molecule.

We find that the mildly chaotropic Rb^+ cation pairs more strongly with the TB e^-_{hyd} and that the TB-Opt electron's water solvation structure is more easily disturbed by the addition of Rb^+-based salts. We also find that both hydrated electron models effectively compete with I^- for pairing with Rb^+, although the TB-Opt model better displaces the I^- ions that are paired with Rb^+. Given that the experimental e^-_{hyd} has a much more positive solvation entropy than iodide,[39,40,45] this suggests that the more chaotropic TB-Opt model provides a better description of the experimental hydrated electron than TB, although even the TB-Opt model could still be too kosmotropic relative to experiment. Our results also provide firm predictions for experiments studying hydrated electrons in the presence of salts with chaotropic cations and different anions. In particular, we predict that the e^-_{hyd}'s absorption spectrum will blue-shift more in Rb^+ (chaotropic) salts than in Na^+ (kosmotropic) salts, and that at high salt concentrations, the blue-shifts will be greater for chaotropic cations paired with kosmotropic anions (e.g., RbF) than for chaotropic cations paired with chaotropic anions (e.g., RbI).

METHODS

As in our previous work,[19−24] we used MQC methods to simulate the hydrated electron's behavior in pure water and in 1 and 3.8 m aqueous RbF and RbI salt solutions. The e^-_{hyd} was simulated quantum mechanically, using both the TB[42] and TB-Opt[11] pseudopotentials to describe its interaction with water. The electron's interactions with the various ions were also described via pseudopotentials developed in-house using the Phillips−Kleinman formalism[46−49]; the details of the development and the actual potentials are given in the Supporting Information (SI). The electron's wave function at each time step was determined from these potentials by solving the time-independent Schrödinger equation on a $24 \times 24 \times 24$ grid, and the wave functions were then used to calculate the force from the electron on the classical particles via the Hellman−Feynman theorem.[50,51]

https://doi.org/10.1021/acs.jpcb.4c04290
J. Phys. Chem. B 2024, 128, 8557−8566

Table 1 summarizes the setup of the different simulations that we chose to run for each electron-water pseudopotential;

Table 1. Setup Parameters for MQC Simulations

[salt]	waters	ions	simulation box length	grid basis length
None	480	0	24.328 Å	17.696 Å
1 m RbF	480	9 each	24.471 Å	17.800 Å
1 m RbI	480	9 each	24.774 Å	18.021 Å
3.8 m RbF	438	30 each	24.133 Å	17.554 Å
3.8 m RbI	438	30 each	25.116 Å	18.269 Å

the parameters are similar to those of our previous work for ease of comparison.[19] We chose the flexible simple point charge model for simulating the water−water interactions[52] and used classical ion−water Lennard−Jones plus Coulomb interactions for Rb^+ and F^- taken from refs 53,54 respectively, with the usual Lorentz−Berthelot combining rules.[55,56] The I^--water Lennard−Jones interactions were described with the same potentials used in our previous work.[19] All of the parameters we used are summarized in the Supporting Information. We also tested other combinations of LJ parameters from various sources,[53,54,57−64] as described in the Supporting Information, and found that although there were quantitative differences, the use of different classical potentials did not change the qualitative trends that we observed.

The number of ions relative to the number of water molecules are calculated based on literature densities at 1 and 3.8 m concentrations.[65]

Following a similar procedure as ref 19, for each system, we first ran all-classical simulations of the various aqueous salt solutions without the quantum mechanical electron in the canonical ensemble (N, V, T) at T = 298 K with the Nosé−Hoover[66] chain thermostat for over a nanosecond to generate equilibrium configurations. We then injected the quantum mechanical electron using both the TB and the TB-Opt pseudopotential models into an equilibrated salt solution configuration. The MQC systems were then further propagated for at least another nanosecond, and we used the last ∼500 ps for analysis. Since both Rb^+ and I^- are heavy and move slowly, we set the masses of these ions to be the same as the mass of water to improve the system equilibration; for this reason, we only report results based on averages over equilibrium configurations and do not investigate any of the system dynamics.

Absorption spectra were calculated following the method used in ref 19. This consisted of calculating the transition dipoles ($\mu_{0,i}$) of the quantum subsystem from the ground (0) to each of the first three excited states (i) for at least 100 uncorrelated (spaced 2 ps apart) equilibrated MQC configurations and binning these by their transition energies ($\Delta E_{0,i}$) into 0.01 eV wide bins according to

$$I(E) = \sum_{i=1}^{3} |\mu_{0,i}|^2 \Delta E_{0,i} \delta(E - \Delta E_{0,i}) \quad (1)$$

The "stick" spectra generated this way were then convoluted with a Gaussian function of width $\sigma = \frac{1}{4\sqrt{2}}$ eV to generate the spectra displayed below.

Potentials of mean force (PMFs) between a single Rb^+ and the e^-_{hyd} were calculated using the coupled-perturbed quantum umbrella sampling method, restraining the distance between the cation and the expectation value of the electron's position.[67,68] Specifically, the Rb^+−e^-_{hyd} distance was restrained from 2.25 to 8 Å in 0.25 Å increments with a quantum harmonic umbrella potential with a 1.5 eV/Å^2 force constant. PMFs between Rb^+ and the different hydrated electron models in the different simulated salt systems were calculated by taking the negative natural logarithm of the corresponding radial distribution function for comparison. We were unable to directly calculate PMFs in high-concentration salt solutions via umbrella sampling because it is not possible to account for situations when distance to one cation is restrained but a different cation moves closer to the e^-_{hyd}.[20]

RESULTS AND DISCUSSION

Our goals in this work are 2-fold. First, we wish to understand the factors that contribute to the blue-shift of the hydrated electron's absorption spectrum in the presence of salt and the nature of any ion pairing that takes place between the e^-_{hyd} and salt cations. Second, we wish to better understand where different simulation models of the hydrated electron sit on the Hofmeister series based on the way they undergo competitive ion pairing, with the hope that future experiments along these lines can start to pin down possible structures for the hydrated electron. In other words, since the mildly chaotropic Rb^+ should pair more strongly with the chaotropic I^- ion than the kosmotropic F^- ion, we can determine where the different hydrated electron models sit on the Hofmeister series by seeing how the e^-_{hyd}'s compete with such anions in pairing with Rb^+.

We start by analyzing the pairing of our chosen electrolyte ions in the absence of an e^-_{hyd}. Figure 1 shows the radial distribution functions, $g(r)$, of anions around Rb^+ in 1 m (panel A) and 3.8 m (panel B) RbF and RbI aqueous solutions. At both salt concentrations, the RbI solutions show a very large first-shell peak near 3.8 Å, indicating a strong degree of contact-ion pairing between these two chaotropic ions; integration of this peak (at 3.8 m) indicates that each Rb^+ is surrounded on average by 2.2 I^- ions. In contrast, RbF solutions show only a tiny first-shell peak near 3 Å with essentially no F^- ions in the first shell of Rb^+, indicating a much weaker pairing for this mixed chaotrope/kosmotrope ion pair. Instead, these solutions show a more intense peak at ∼4.5 Å, indicating that Rb^+ and F^- form only some solvent-separated ion pairs. This pairing behavior of both solutions is as expected given the relative positions of these ions on the Hofmeister series.

We next analyzed the pairing of our chosen Rb^+ electrolyte cation and the different hydrated electron models in the absence of anions. Figure 2 shows the potentials of mean force (PMFs) between a single Rb^+ ion and the expectation value of the e^-_{hyd}'s position, with the zero of energy arbitrarily defined at the farthest electron-cation distance. The PMF minima occur around separations of 4.53 and 5.01 Å for the TB and TB-Opt electron models, respectively, in agreement with the radial distribution functions presented in Figure S4 in the Supporting Information. Previous studies with sodium and calcium salts show that the TB e^-_{hyd} forms contact-ion pairs (CIPs) with the salt cation.[19] In the case of Rb^+, we do not see CIP formation with either e^-_{hyd} model. Based on their respective diameters, the expected contact pairing distance for Rb^+ and a e^-_{hyd} should be 3.57 Å for the TB model and 3.63 Å for the TB-Opt model, as indicated by the green arrow in Figure 2. Since the actual minima are much farther than this, the PMFs suggest that both

https://doi.org/10.1021/acs.jpcb.4c04290
J. Phys. Chem. B 2024, 128, 8557−8566

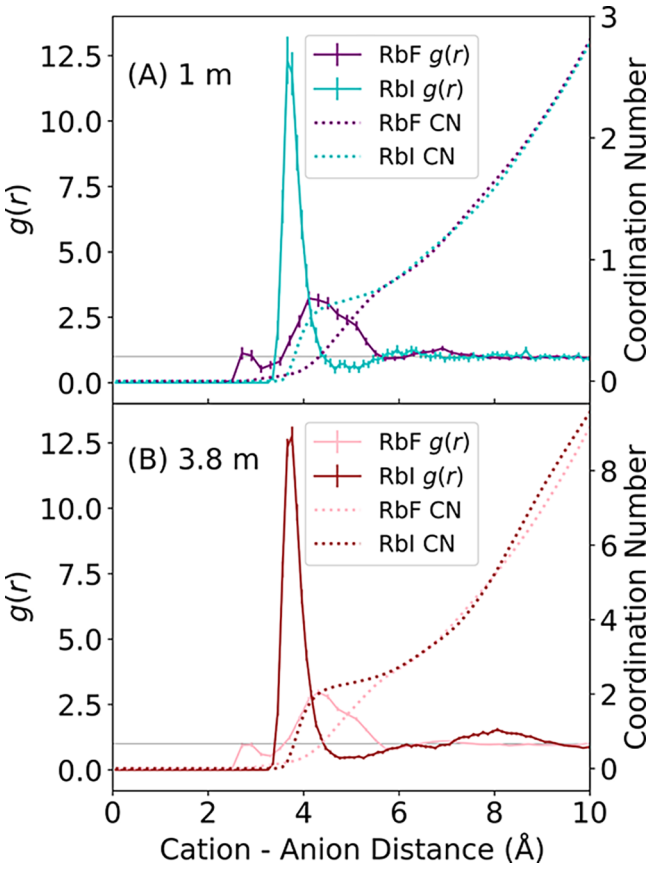

Figure 1. Classically simulated (with no e^-_{hyd}) Rb^+-anion radial distribution functions, $g(r)$ (left axis), and running coordination number (right axis) in 1 m aqueous RbF/RbI (A) and 3.8 m aqueous RbF/RbI (B). In agreement with expectations from the Hofmeister series and chaotrope/kosmotrope pairing, Rb^+ (a mild chaotrope) forms many more contact pairs with I^- (a chaotrope) than with F^- (a kosmotrope) at both salt concentrations. There are ∼0 first-shell F^- around Rb^+ at both concentrations, while there are ∼0.65 first-shell I^- around Rb^+ in 1 m RbI and ∼2.2 in 3.8 m RbI (see the Supporting Information for more details on coordination numbers).

e^-_{hyd} models form solvent-separated pairs with Rb^+. Furthermore, radial distribution functions shown in Figure S4 in the Supporting Information indicate that there is a clear solvation shell of water immediately surrounding both electron models for both salt systems at each concentration.

Another feature of the PMFs in Figure 2 is that both e^-_{hyd} models show generally similar free energies of interaction with Rb^+, $-2.6\ k_BT$ for TB and $-2.0\ k_BT$ for TB-Opt. This is quite unlike the case with Na^+, where the Na^+−TB electron interaction is $4.5\ k_BT$ deeper than the Na^+−TB-Opt interaction.[22,36] The weaker overall attraction and the similarity of the two electron models' behavior with Rb^+ result from the fact that solvent-separated ion pairs generally have weaker interactions.[20,22] However, the equilibrium cation-electron distance is ∼0.5 Å greater for the TB-Opt electron than the TB e^-_{hyd} with both the Na^+ and Rb^+ cations,[22] indicative of a stronger interaction for TB and thus suggesting that the TB electron falls in a more similar position on the Hofmeister series to these ions than does the TB-Opt e^-_{hyd}.

Armed with an understanding of the cation−anion and cation-electron interactions in our chosen systems, we next examine the effect of adding RbF and RbI salts on the different model hydrated electrons' absorption spectra. Figure 3A−D

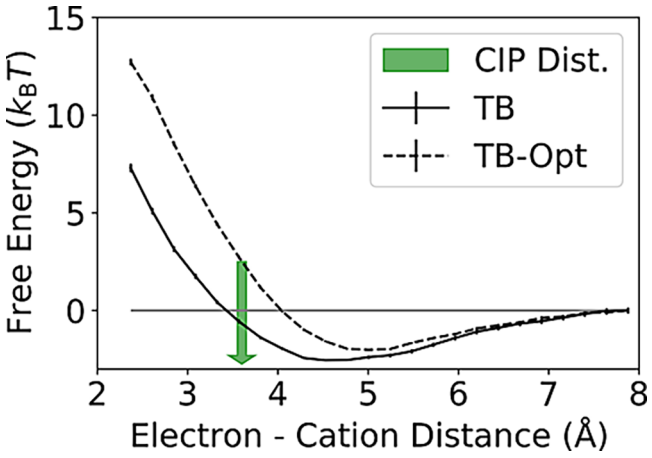

Figure 2. Potentials of mean force (PMFs) between a single Rb^+ and the centers of mass of the TB/TB-Opt e^-_{hyd}'s, calculated following ref 67. The minimum potential energy occurs around 4.5−5 Å, although the expected contact-ion pair (CIP) distance is slightly over 1 Å closer than the minimum (green arrow), indicating that the minimum corresponds to solvent-separated cation-electron pairs. Figure S5 in the Supporting Information shows that as the salt concentration increases, the energy well between Rb^+ and the TB e^-_{hyd} gets shallower, consistent with results in ref 20.

shows the calculated absorption spectra of both the TB (solid curves, panels A and C) and TB-Opt (dashed curves, panels B and D) e^-_{hyd} models in both pure water and the various Rb^+ salt solutions. As seen in both experiments and simulations with other electrolytes,[19−22,26,36] the data show that the absorption spectrum of both electron models blue-shifts with added salt without a significant change in shape, suggesting that the simulations are indeed capturing at least some aspects of the experimental system.

The magnitude of the salt-induced spectral blue-shift for the TB electron (Figure 3A,C) is significantly smaller than that seen in our previous simulation work with NaCl and $CaCl_2$.[19] For example, the TB electron's spectrum shifts ∼750 meV to the blue in 1 m NaCl[19] but only ∼150 meV in 1 m RbF; this is another indication that the TB e^-_{hyd} forms only solvent-separated pairs with Rb^+ instead of CIPs with more kosmotropic cations. Moreover, the magnitude of the spectral shift does not saturate with increasing salt concentration in the Rb^+ salt solutions in the same way it does in Na^+ and Ca^{2+} solutions[20] or experimentally:[26] the shift is larger from 1 to 3 m than from 0 to 1 m. This suggests that each cation that (solvent-separately) pairs with the TB e^-_{hyd} contributes roughly equally to the spectral shift, emphasizing that ion pairing of hydrated electrons is fundamentally different with chaotropic cations like Rb^+ than with the kosmotropic cations that were studied previously.[19−24]

The TB-Opt e^-_{hyd}'s spectral behavior, as shown in Figure 3B,D, is also different from previous work with Na^+. Noting that the TB-Opt electron's spectrum in pure water is ∼200 meV redder than that of the TB e^-_{hyd},[11] we see that the TB-Opt electron experiences slightly larger relative spectral shifts in the presence of Rb^+ than the TB electron, which is a different behavior than we previously observed with Na^+.[22] The fact that TB e^-_{hyd}'s absorption spectrum is affected more by Na^+ and the TB-Opt is affected more by Rb^+ suggests that the TB electron is more kosmotropic than the TB-Opt electron. As the strongly positive experimental solvation entropy of the e^-_{hyd} indicates that it is highly chaotropic,[39,40] this suggests that the TB-Opt

https://doi.org/10.1021/acs.jpcb.4c04290
J. Phys. Chem. B 2024, 128, 8557−8566

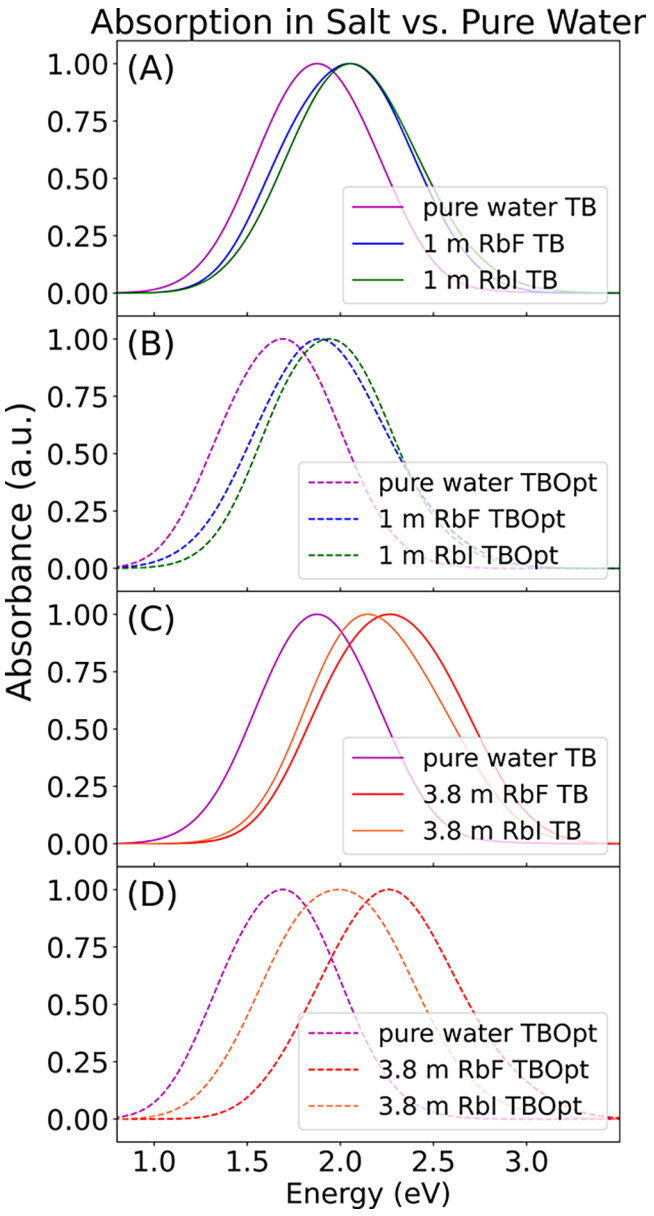

Figure 3. Simulated absorption spectra of the TB hydrated electron (solid curves) in 1 m salt solutions (A), the TB-Opt hydrated electron (dashed curves) in 1 m salt solutions (B), the TB e^-_{hyd} in 3.8 m salt solutions (C), and the TB-Opt e^-_{hyd} in 3.8 m salt solutions (D). The purple curves show the spectra of the different electron models in pure water for comparison. The general shape of the absorption spectra is about the same for the simulated systems, and the trends in the peak shifts of the absorption spectra are summarized in Figure 4A below.

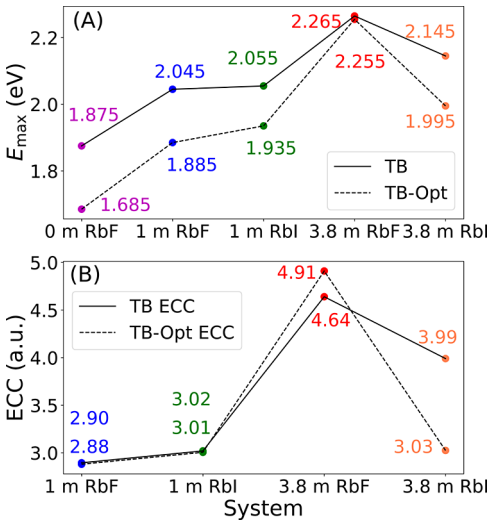

Figure 4. Absorption spectra peak energies of the TB (solid lines) and TB-Opt (dashed lines) e^-_{hyd} models in each of the eight salt systems (A), and effective cation charge model predictions of the relative absorption peaks in the same salt systems (B). The effective cation charge model predictions generally agree with the simulated trends, predicting that compared to the e^-_{hyd} in pure water, 1 m RbI produces a slightly greater blue-shift than RbF, but 3.8 m RbF produces a much greater blue-shift than RbI; the model also captures the fact that as concentration increases for both salts, the absorption blue-shift is greater.

model likely has a higher solvation entropy than TB and thus is in better agreement with experiment.

Figure 4A summarizes how the absorption maxima of the different e^-_{hyd} models' spectra shift in the presence of different concentrations of RbF and RbI. In the 3.8 m salt systems, RbF blue-shifts the absorption spectra of both electron models more than RbI, but in the 1 m solutions, RbF blue-shifts the spectra slightly less than RbI. This is a clear signature of competitive ion pairing, where concentration-dependent changes in the cation:anion interactions affect how the cations can in turn interact with the different hydrated electron models. Below, we propose a model, summarized in Figure 4B, that is able to roughly explain the observed spectral trends with both anion identity and salt concentration.

To better understand the competitive ion pairing behavior with the different Rb^+ salts and concentrations, we examined the number of cations and anions present in the vicinity of the different e^-_{hyd} models. Figure 5 shows a "heat map" of the number of cations present in the first (solvent-separated) shell of the TB (left panels) and TB-Opt (right panels) electrons against the number of the first-shell anions around only those cations. The way we define the first-shell cutoffs for each system from the corresponding radial distribution functions is described in detail in the Supporting Information.

The thin blue lines on the "heat maps" in Figure 5 display the average total number of the solvent-separated Rb^+'s around the different e^-_{hyd}'s and the average total number of anions around those Rb^+ cations, allowing us to divide the two to obtain the number of anions per first-shell cation. The results of this calculation are summarized in Table 2. For example, for the 1 m RbF system, there are typically 3.83 Rb^+ around the TB e^-_{hyd} (blue horizontal line) and a total of 0.11 F^- around all of these Rb^+, yielding 0.03 F^- around each first-shell Rb^+.

Figure 5 and Table 2 help us gain insights into where the different paired species in our simulations sit relative to each other on the Hofmeister series. First, we see that there are generally more Rb^+ cations around the different e^-_{hyd} models in the RbF systems than RbI systems, indicating that both electron models out-compete F^- more than I^- in pairing with Rb^+. Based on the idea that ions that are similarly positioned on the Hofmeister series have the strongest tendency to pair, this suggests that our simulated I^- is in a similar Hofmeister series position as Rb^+ and more chaotropic than F^-. Next, we find that the TB and TB-Opt e^-_{hyd}'s have very different local environments in the same salt system: the TB electron generally has more Rb^+ in its first solvent-separated shell than

https://doi.org/10.1021/acs.jpcb.4c04290
J. Phys. Chem. B 2024, 128, 8557−8566

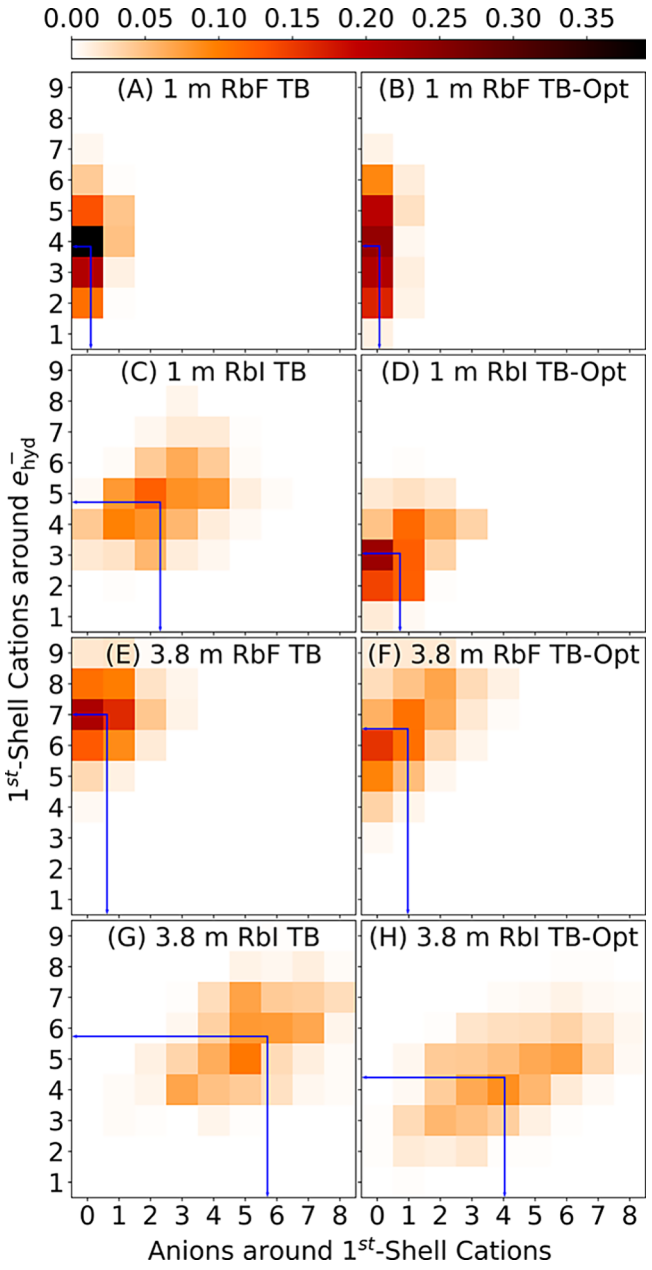

Figure 5. Heat maps, normalized by total density, showing cation and anion distributions near the different e^-_{hyd} models in 1 m (panels A–D) and 3.8 m (panels E–H) salt solutions: the *y*-axis shows the number of Rb^+'s one solvent shell away from the e^-_{hyd}, while the *x*-axis reflects the total number of first-shell anions around those Rb^+'s. Thin blue lines denote the average values along each axis for the respective systems. For all systems, the number of Rb^+'s near both electrons increases as the salt concentration increases. For both e^-_{hyd} models, the number of anions per first-shell Rb^+ is similar for RbF, but the Rb^+'s near the TB electron are more strongly paired with I^- at both concentrations compared to the TB-Opt electron.

Table 2. Average Total Number of Anions around First-Shell Rb^+ Cations, Average Total Number of First-Shell Rb^+'s in Solvent-Separated Pairs with the Different e^-_{hyd} Models, and Their Quotient, the Average Number of Anions per First-Shell Rb^+

system	total anions around 1st-shell Rb^+	total Rb^+ around e^-_{hyd}	anion per 1st-shell Rb^+
1 m RbF TB	0.11	3.83	0.03
1 m RbF TB-Opt	0.07	3.85	0.02
1 m RbI TB	2.31	4.72	0.49
1 m RbI TB-Opt	0.72	3.05	0.24
3.8 m RbF TB	0.63	7.00	0.09
3.8 m RbF TB-Opt	0.97	6.54	0.15
3.8 m RbI TB	5.71	5.73	1.00
3.8 m RbI TB-Opt	4.04	4.40	0.92

ordering, we next examined how the TB and TB-Opt electron hydration structures are altered upon the addition of salt and the formation of solvent-separated ion pairs. Figure 6 shows

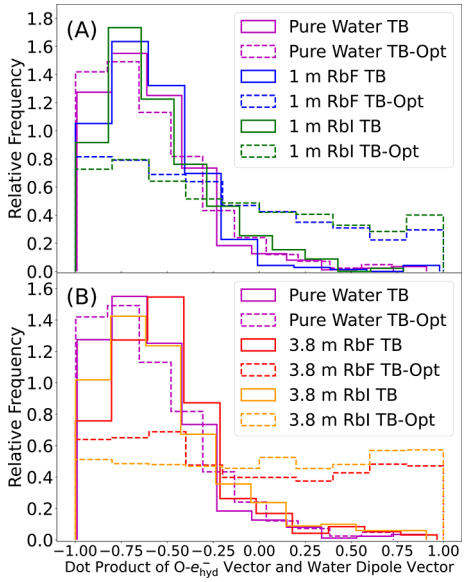

Figure 6. Water solvation orientational structure around the TB (solid lines) and TB-Opt (dashed lines) e^-_{hyd} models, characterized as a dot product between a unit vector connecting the electron center-of-mass to a first-shell water O atom and a unit vector along that water's dipole. The purple traces in both panels show the distributions for both the TB (solid trace) and TB-Opt (dashed trace) electron models in pure water for reference, showing that both models are predominantly solvated by water H-bonds. Upon the addition of salt, the TB e^-_{hyd} (solid traces) maintains its local solvation structure, but the TB-Opt e^-_{hyd} (dashed traces) does not, whether at 1 m salt (panel A) or 3.8 m salt (panel B). The greater disruption of the TB-Opt e^-_{hyd}'s solvation structure correlates well with the fact that its spectral shift (Figure 4A) is larger.

the TB-Opt electron, particularly in the RbI solutions. This suggests that the TB electron model is in a Hofmeister position similar to that of Rb^+, leading to more favorable pairing, which is consistent with the PMF in Figure 2, which shows that TB e^-_{hyd}–Rb^+ interactions have a deeper free energy well than TB-Opt e^-_{hyd}–Rb^+ interactions.

To take a step further in elucidating how chaotropic the two e^-_{hyd} models are and determining their Hofmeister series the orientational distribution of the first-shell water molecules around the different hydrated electron models in each electrolyte solution. The *x*-axis is defined as the dot product between a unit vector connecting the water O atom to the center-of-mass of the e^-_{hyd} and a unit vector along that water's dipole. With the way we define the dipole, a value of −1 means that the two H atoms point toward the electron's center, a value of +1 means the O end of water points toward the e^-_{hyd},

https://doi.org/10.1021/acs.jpcb.4c04290
J. Phys. Chem. B 2024, 128, 8557–8566

and a value of ∼ −0.7 means that a water H-bond is directed toward the electron's center.

The purple traces in Figure 6 show the water orientation around the simulated e^-_{hyd} in pure water; the peak near −0.7 indicates that the predominant first-shell solvation motif for both models is via water H-bond donation. Upon the addition of salt, the water structure around the TB-Opt e^-_{hyd} (dashed traces) is significantly disturbed, to the point where at the 3.8 m salt concentration, there is essentially no preferred first-shell water orientation with either salt. In contrast, the TB e^-_{hyd} (solid traces) shows no change in its local hydration structure within error when salt is added. The fact that Rb^+ cations can disrupt the solvation structure of TB-Opt electrons but not TB electrons indicates that the TB-Opt e^-_{hyd} is much more chaotropic than Rb^+, while the TB e^-_{hyd} is more kosmotropic than Rb^+. The fact that the local hydration structure is so strongly disrupted explains why the TB-Opt electron generally shows a greater absorption spectral shift than the TB electron in Figure 4A, even though the TB-Opt electron generally has fewer salt cations in the solvent-separated ion pairs.

This observation of how Rb^+ salts affect simulated e^-_{hyd}'s is quite different from our previous work, where we saw that the TB electron's solvation structure was disrupted upon formation of contact pairs with Na^+, while the TB-Opt electron's structure was generally unaffected.[22] This difference arises because Na^+ is more kosmotropic than the TB e^-_{hyd} so that when these two species are in a contact pair, the Na^+ determines the net orientation of the water molecules that reside in the first shells of both species.[21] This allows us to pin down the position of the TB e^-_{hyd} on the Hofmeister series as somewhere between that of Na^+ and Rb^+, a result that does not fit well with the fact that the experimental solvation entropy of the hydrated electron is much larger than that of Rb^+.[39,40,45] We also previously found that the softer cavity and more fluxional structure of the TB-Opt e^-_{hyd} allows the proximal water molecules to solvate both the electron and Na^+ relatively well.[22] (We note that e^-_{hyd}'s simulated by DFT[69] actually disrupt the hydration structure of paired Na^+, indicating that DFT-simulated hydrated electrons are even more kosmotropic than Na^+, in sharp contrast to experiment).[22,23] Here, the fact that even in a solvated-separated pair, Rb^+ can disrupt the solvation structure of the TB-Opt electron indicates that the TB-Opt electron lies to the chaotropic side of Rb^+ on the Hofmeister series.

By combining this insight with our previous work, we can order all of our simulated ions along the Hofmeister series. Not surprisingly, F^- is the most kosmotropic out of all the species in this simulation study and our previous work.[19−22] Based on its ion pairing behavior, Rb^+ is in a roughly similar position as I^- on the Hofmeister series. Rb^+ is also similarly chaotropic compared with the TB electron and less chaotropic than the TB-Opt electron. Thus, based on the observed competitive pairing and which ions disrupt the hydration structure of the others, we can estimate the relative positions of the different species on the Hofmeister series (from most kosmotropic to most chaotropic) as follows:

$$F^- << I^- \leq \text{TB } e^-_{hyd} \leq Rb^+ < \text{TB-Opt } e^-_{hyd} \quad (2)$$

Given that the e^-_{hyd} has the highest solvation entropy and is thus the most chaotropic of the simple ions,[39,40,45] our simulations thus indicate that the more chaotropic TB-Opt electron model matches better with experiment than the TB model, although it still is not likely chaotropic enough.

We note that as of this writing, no experiments have been performed measuring the spectrum of the hydrated electrons in salt solutions with chaotropic cations and different anions, so this work provides an experimental prediction that can be directly tested. Based on the above reasoning, we predict that the experimental results should mirror the trends seen with the TB-Opt e^-_{hyd} model more than the TB e^-_{hyd} model. In previous work, we found that the TB-Opt model showed a spectral blue-shift of ∼70 meV in ∼1 m aqueous Na^+ solutions,[22] a result in reasonable agreement with experiments at higher salt concentrations.[26] Here, we predict a larger spectral blue-shift of ∼200 meV under similar conditions for Rb^+ salts. Furthermore, the experiments that measured the e^-_{hyd}'s absorption spectrum in electrolyte solutions used salts with kosmotropic cations and kosmotropic anion, kosmotropic cation and chaotropic anions, and chaotropic cations and kosmotropic anions;[26] thus, we also predict that experiments using chaotropic cation salts will show a greater spectral blue-shift for kosmotropic counterions (like F^-) than chaotropic counterions (like I^-) due to competitive ion pairing.

With a better understanding of where different e^-_{hyd} models sit on the Hofmeister series, we can return to analyzing how competitive ion pairing determines the observed spectral shifts. Specifically, the data in Figure 5 and Table 2 can be used to rationalize the spectroscopic trends observed in Figures 3 and 4A. We find that the total number of Rb^+ cations in the first (solvent-separated) shell of both e^-_{hyd} models correlates well with the observed concentration-dependent trends in the spectral shifts for both salts. We also see, however, that the number of anions near those cations also needs to be considered to explain the finer details of the spectral shifts, such as why at 1 m salt concentration, the difference between the spectral blue-shifts in RbI and RbF is smaller than that at 3.8 m for both hydrated electron models.

There are about the same number of F^- and I^- ions around each first-shell Rb^+ in 1 m RbF and RbI, respectively, leading to similar blue-shifts of the TB and TB-Opt e^-_{hyd} spectra in the 1 m salt solutions. On the other hand, there are many more I^- than F^- around each first-shell Rb^+ at 3.8 m, leading to much larger spectral blue-shifts for both hydrated electron models in 3.8 m RbF than 3.8 m RbI, where the effect of the cations in RbI on the electrons is "mitigated" by all the nearby anions. We observed a similar effect with kosmotropic cation salts and the TB e^-_{hyd} in our previous work,[19] and the data here indicate that this type of competitive ion pairing also holds for chaotropic cation salts as well as for the TB-Opt e^-_{hyd} model.

To summarize the effect of competitive ion pairing on the observed spectral shifts of the different e^-_{hyd} models, we developed an effective cation charge (ECC) model that describes the effective charge of Rb^+ cations in solvent-separated pairs felt by the electron, taking into account shielding by the anions and the relative distances of all of the ions. We choose a relatively simple model for this:

$$\text{ECC} = \sum_{i=1}^{N} \frac{q_i}{d_i} \quad (3)$$

where N is the total number of ions surrounding the e^-_{hyd}, and q_i is the charge of each ion. Here, d_i is a discretized distance that can take on one of three values: 1, 2, or ∞, as illustrated in Figure 7. The idea is that the e^-_{hyd} feels the full charge of any

https://doi.org/10.1021/acs.jpcb.4c04290
J. Phys. Chem. B 2024, 128, 8557−8566

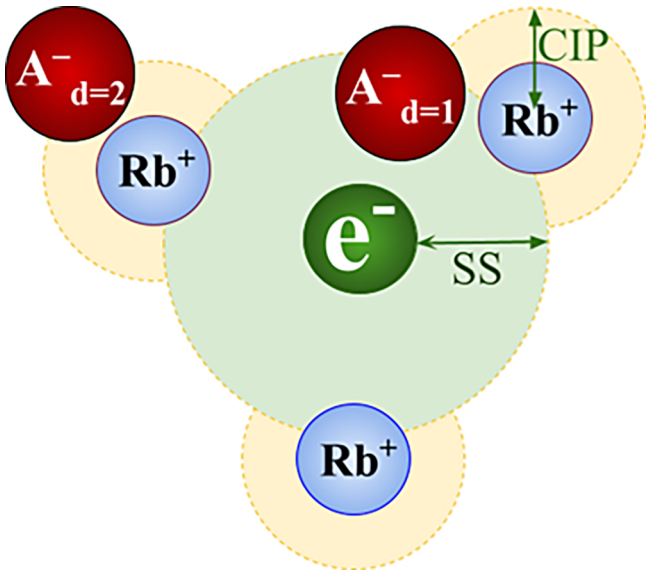

Figure 7. Illustration of d_i values in the ECC, eq 3. $d_i = 1$ if the ion is within the first solvent-separated shell of the electron (SS), inside the green shaded region; the red anion sphere labeled $A^-_{d=1}$ is an example. $d_i = 2$ if the anion is within the first shell of Rb^+ (CIP) but not within SS (inside shaded yellow regions); the red anion sphere labeled $A^-_{d=2}$ is an example. $d_i = \infty$ if the ion is far from both the electron and its first solvent-separated shell of Rb^+ (white space outside the figure). The SS and CIP distances are determined by the corresponding radial distribution function and are summarized in the Supporting Information.

solvent-separated paired Rb^+ ions that are not also paired with salt anions but only feels half of the charge of solvent-separated paired Rb^+ ions that are also paired with salt anions far from the electron. Finally, anions closer to the e^-_{hyd} than Rb^+ completely screen the Rb^+'s cationic charge from the e^-_{hyd}.

Figure 4B shows that the ECC for both e^-_{hyd} models in the different salt solutions has a very similar pattern as the calculated spectral shifts in Figure 4A. In our previous work, studying hydrated electron pairing with kosmotropic cations, we were able to rationalize the observed spectral shifts using only the number of cations near the e^-_{hyd} and number of anions around those cations.[19] However, to accurately explain our observations with the chaotropic Rb^+ salts studied here, we find that we must distinguish between anions that are close to only the first-shell cations and anions that are close to both the first-shell cations and e^-_{hyd}. This is because Rb^+ and the e^-_{hyd} form only solvent-separated pairs, allowing anions to get as close (and occasionally closer) to the electron as the cations, something that we did not observe with Na^+ or Ca^{2+}.[19] In this SI, we show other attempts to rationalize the calculated spectral shifts that did not work as well as the ECC model. The fact that the ECC model is more complex than what we saw in our previous work indicates that changing the position of the cation on the Hofmeister series fundamentally changes the ion-pairing relationships and, thus, the hydration and ion solvation structures around the different e^-_{hyd} models.

CONCLUSIONS

In summary, we analyzed how two different e^-_{hyd} models, TB and TB-Opt, interact with various concentrations of RbF and RbI aqueous salt solutions. For all of the systems we studied, the mildly chaotropic Rb^+ ion and electron form only solvent-separated pairs, with the closest cation:e^-_{hyd} interaction being at least one water molecule apart. This leads to an overall weaker interaction than that observed for hydrated electrons in direct CIPs with kosmotropic cations,[19−23] as indicated by the e^-_{hyd}:Rb^+ PMFs seen in Figure 2.

Based on the extent of competitive ion pairing between the charged species in the different systems that we examined, we find that both e^-_{hyd} models out-compete F^- more than I^- in the pairing with Rb^+ in 3.8 m, indicating that the chaotrope/kosmotrope ion pairing strengths based on the Hofmeister series also apply to chaotropic cation salt solutions. This leads to RbF having a stronger cation:e^-_{hyd} interaction with both electron models because RbF has a weaker cation:anion interaction. As a consequence, we predict that salts with chaotropic cations and komsotropic anions should produce larger blue-shifts in the e^-_{hyd}'s absorption spectrum than salts with other cation/anion combinations. These ideas are consistent with previous simulation work that explains why larger blue-shifts are observed with stronger (cation:e^-_{hyd}) interactions.[19−22] We also predict a stronger concentration dependence for the spectral blue-shift with chaotropic cations compared to that with kosmotropic cations.

We also examined the hydration structures around the e^-_{hyd} and found that electrolytes with chaotropic cations disturb the solvation structure of the TB-Opt electron much more than the TB electron, resulting in the former's absorption spectrum having greater shifts. By looking at the spectral shifts, degree of ion pairing, and how the paired ions disrupt each others' hydration spheres, we were able to roughly place all of the ions in our simulations on the Hofmeister series, as summarized in eq 2. Importantly, we conclude that the TB-Opt electron is more chaotropic than the TB electron (which is also more kosmotropic than Rb^+), suggesting that the structure of the TB-Opt electron is closer to experiment given that it is known experimentally that the e^-_{hyd} is a champion chaotrope.[39,40]

Since previous work shows that TB-Opt electron's predicted absorption spectrum shift in the presence of ions is much closer to experiment than either the TB model or DFT-based simulations,[22] we predict that the greater spectral blue-shift of the TB-Opt e^-_{hyd} with Rb^+ (chaotropic) salts compared to Na^+ (kosmotropic) salts that we see should also be observed experimentally, and we hope this work inspires experimentalists to perform exactly this comparison. We note that previous experiments studying Cl^- salts found that the more chaotropic Cs^+ indeed produced a greater blue-shift of the electron's spectrum than the more kosmotropic Na^+,[26] consistent with our simulations, which also suggest that there should be a smaller induced shift for salts with both chaotropic cations and anions. Overall, given that there are no easy ways to directly measure the solvation structure of hydrated electrons, we believe that studying the way they undergo ion pairing with electrolytes whose ions have different positions on the Hofmeister series provides a strong indirect route to understanding the molecular nature of the e^-_{hyd}.

ASSOCIATED CONTENT

Supporting Information

The Supporting Information is available free of charge at https://pubs.acs.org/doi/10.1021/acs.jpcb.4c04290.

Pseudo-orbital/pseudopotential calculations, additional radial distribution functions and PMFs, lists of

https://doi.org/10.1021/acs.jpcb.4c04290
J. Phys. Chem. B 2024, 128, 8557−8566

parameters used, additional water orientation analysis, and inaccurate model for comparison (PDF)

AUTHOR INFORMATION

Corresponding Author

Benjamin J. Schwartz − *Department of Chemistry & Biochemistry, University of California, Los Angeles, Los Angeles, California 90095-1569, United States;* orcid.org/0000-0003-3257-9152; Phone: (310) 206-4113; Email: schwartz@chem.ucla.edu

Authors

Hannah Y. Liu − *Department of Chemistry & Biochemistry, University of California, Los Angeles, Los Angeles, California 90095-1569, United States*

Kenneth J. Mei − *Department of Chemistry & Biochemistry, University of California, Los Angeles, Los Angeles, California 90095-1569, United States*

William R. Borrelli − *Department of Chemistry & Biochemistry, University of California, Los Angeles, Los Angeles, California 90095-1569, United States*

Complete contact information is available at: https://pubs.acs.org/10.1021/acs.jpcb.4c04290

Notes

The authors declare no competing financial interest.

ACKNOWLEDGMENTS

This work was supported by the National Science Foundation under grants CHE-1856050 and CHE-2247583. Computational resources were provided by the UCLA Institute for Digital Research and Education.

REFERENCES

(1) Hart, E. J.; Boag, J. W. Absorption Spectrum of the Hydrated Electron in Water and in Aqueous Solutions. *J. Am. Chem. Soc.* **1962**, *84*, 4090−4095.

(2) Kevan, L. Solvated Electron Structure in Glassy Matrixes. *Acc. Chem. Res.* **1981**, *14*, 138−145.

(3) Naiayana, M.; Kevan, L. J. Electron spin echo modulation study of the geometry of solvated electrons in ethanol glass: An example of a molecular dipole oriented solvation shell. *Chem. Phys.* **1980**, *72*, 2891−2892.

(4) Ichikawa, T.; Kevan, L. J. Electron spin echo modulation studies of tetracyanoethylene anion solvation in methanol, acetone, and dimethylsulfoxide: Evidence for molecular dipole oriented solvation shells around large anions. *J. Chem. Phys.* **1980**, *72*, 2295−2299.

(5) Kevan, L.; Ichikawa, T.; Ichikawa, T. Structure of solvated electrons in 3-methylpentane glass. Second-moment electron spin resonance analysis of specifically deuterated 3-methylpentanes. *J. Phys. Chem.* **1980**, *84*, 3260−3263.

(6) Sauer, M. C.; Shkrob, I. A.; Lian, R.; Crowell, R. A.; Bartels, D. M.; Chen, X.; Suffern, D.; Bradforth, S. E. Electron Photodetachment from Aqueous Anions. 2. Ionic Strength Effect on Geminate Recombination Dynamics and Quantum Yield for Hydrated Electron. *J. Phys. Chem. A* **2004**, *108*, 10414−10425.

(7) Janik, I.; Lisovskaya, A.; Bartels, D. M. Partial Molar Volume of the Hydrated Electron. *J. Phys. Chem. Lett.* **2019**, *10*, 2220−2226.

(8) Asaad, A. N.; Chandrasekhar, N.; Nashed, A. W.; Krebs, P. Is There Any Effect of Solution Microstructure on the Solvated Electron Absorption Spectrum in LiCl/H 2 O Solutions? *J. Phys. Chem. A* **1999**, *103*, 6339−6343.

(9) Turi, L.; Borgis, D. Analytical Investigations of an Electron-Water Molecule Pseudopotential. II. Development of a New Pair Potential and Molecular Dynamics Simulations. *J. Chem. Phys.* **2002**, *117*, 6186−6195.

(10) Larsen, R. E.; Glover, W. J.; Schwartz, B. J. Does the Hydrated Electron Occupy a Cavity? *Science* **2010**, *329*, 65−69.

(11) Glover, W. J.; Schwartz, B. J. Short-Range Electron Correlation Stabilizes Noncavity Solvation of the Hydrated Electron. *J. Chem. Theory Comput.* **2016**, *12*, 5117−5131.

(12) Schnitker, J.; Rossky, P. J. An Electron-Water Pseudopotential for Condensed Phase Simulation. *J. Chem. Phys.* **1987**, *86*, 3462−3470.

(13) Uhlig, F.; Marsalek, O.; Jungwirth, P. Unraveling the complex nature of the hydrated electron. *J. Phys. Chem. Lett.* **2012**, *3*, 3071−3075.

(14) Ambrosio, F.; Miceli, G.; Pasquarello, A. Electronic Levels of Excess Electrons in Liquid Water. *J. Phys. Chem. Lett.* **2017**, *8*, 2055−2059.

(15) Park, S. J.; Schwartz, B. J. Evaluating Simple Ab Initio Models of the Hydrated Electron: The Role of Dynamical Fluctuations. *J. Phys. Chem. B* **2020**, *124*, 9592−9603.

(16) Shen, Z.; Peng, S.; Glover, W. J. Flexible Boundary Layer Using Exchange for Embedding Theories. II. QM/MM Dynamics of the Hydrated Electron. *J. Chem. Phys.* **2021**, *155*, 224113.

(17) Wilhelm, J.; VandeVondele, J.; Rybkin, V. Dynamics of the Bulk Hydrated Electron from Many-Body Wave-Function Theory. *Angew. Chem., Int. Ed.* **2019**, *58*, 3890−3893.

(18) Jou, F. Y.; Freeman, G. R. Temperature and isotope effects on the shape of the optical absorption spectrum of solvated electrons in water. *J. Phys. Chem.* **1979**, *83*, 2383−2387.

(19) Narvaez, W. A.; Park, S. J.; Schwartz, B. J. Competitive Ion Pairing and the Role of Anions in the Behavior of Hydrated Electrons in Eletrolytes. *J. Phys. Chem. B* **2022**, *126*, 7701−7708.

(20) Narvaez, W. A.; Park, S. J.; Schwartz, B. J. Hydrated Electrons in High-Concentration Electrolytes Interact with Multiple Cations: A Simulation Study. *J. Phys. Chem. B* **2022**, *126*, 3748−3757.

(21) Park, S. J.; Narvaez, W. A.; Schwartz, B. J. How Water-Ion Interactions Control the Formation of Hydrated Electron:Sodium Cation Contact Pairs. *J. Phys. Chem. B* **2021**, *125*, 13027−13040.

(22) Park, S. J.; Narvaez, W. A.; Schwartz, B. J. Ab Initio Studies of Hydrated Electron/Cation Contact Pairs: Hydrated Electrons Simulated with Density Functional Theory Are Too Kosmotropic. *J. Phys. Chem. Lett.* **2023**, *14*, 559−566.

(23) Park, S. J.; Schwartz, B. J. How Ions Break Local Symmetry: Simulations of Polarized Transient Hole Burning for Different Models of the Hydrated Electron in Contact Pairs with Na^+. *J. Phys. Chem. Lett.* **2023**, *14*, 3014−3022.

(24) Narvaez, W. A.; Wu, E. C.; Park, S. J.; Gomez, M.; Schwartz, B. J. Trap-Seeking or Trap-Digging? Photoinjection of Hydrated Electrons into Aqueous NaCl Solutions. *J. Phys. Chem. Lett.* **2022**, *13*, 8653−8659.

(25) Lin, M.; Kumagai, Y.; Lampre, I.; Coudert, F.-X.; Muroya, Y.; Boutin, A.; Mostafavi, M.; Katsumura, Y. Temperature Effect on the Absorption Spectrum of the Hydrated Electron Paired with a Lithium Cation in Deuterated Water. *J. Phys. Chem. A* **2007**, *111*, 3548−3553.

(26) Bonin, J.; Lampre, I.; Mostafavi, M. Absorption Spectrum of the Hydrated Electron Paired with Nonreactive Metal Cations. *Radiat. Phys. Chem.* **2005**, *75*, 288−296.

(27) Bonin, J.; Lampre, I.; Soroushian, B.; Mostafavi, M. First Observation of Electron Paired with Divalent and Trivalent Nonreactive Metal Cations in Water. *J. Phys. Chem. A* **2004**, *108*, 6817−6819.

(28) Assel, M.; Laenen, R.; Laubereau, A. Dynamics of Excited Solvated Electrons in Aqueous Solution Monitored with Femtosecond-Time and Polarization Resolution. *J. Phys. Chem. A* **1998**, *102*, 2256−2262.

(29) Cavanagh, M. C.; Larsen, R. E.; Schwartz, B. J. Watching Na Atoms Solvate into (Na^+, e^-) Contact Pairs: Untangling the Ultrafast Charge-Transfer-to-Solvent Dynamics of Na-in Tetrahydrofuran (THF). *J. Phys. Chem. A* **2007**, *111*, 5144−5157.

(30) Glover, W. J.; Larsen, R. E.; Schwartz, B. J. First principles multielectron mixed quantum/classical simulations in the condensed phase. II. The charge-transfer-to-solvent states of sodium anions in liquid tetrahydrofuran. *J. Chem. Phys.* **2010**, *132*, 144102.
(31) Mani, T.; Grills, D. C.; Miller, J. R. Vibrational Stark Effects To Identify Ion Pairing and Determine Reduction Potentials in Electrolyte-Free Environments. *J. Am. Chem. Soc.* **2015**, *137*, 1136−1140.
(32) Hack, J.; Grills, D. C.; Miller, J. R.; Mani, T. Identification of Ion-Pair Structures in Solution by Vibrational Stark Effects. *J. Phys. Chem. B* **2016**, *120*, 1149−1157.
(33) Wu, Q.; Zaikowski, L.; Kaur, P.; Asaoka, S.; Gelfond, C.; Miller, J. R. Multiply Reduced Oligofluorenes: Their Nature and Pairing with THF-Solvated Sodium Ions. *J. Phys. Chem. C* **2016**, *120*, 16489−16499.
(34) Bird, M. J.; Iyoda, T.; Bonura, N.; Bakalis, J.; Ledbetter, A. J.; Miller, J. R. Effects of electrolytes on redox potentials through ion pairing. *J. Electroanal. Chem.* **2017**, *804*, 107−115.
(35) Marasas, R. A.; Iyoda, T.; Miller, J. R. Benzene Radical Ion in Equilibrium with Solvated Electrons. *J. Phys. Chem. A* **2003**, *107*, 2033−2038.
(36) Coudert, F.-X.; Archirel, P.; Boutin, A. Molecular Dynamics Simulations of Electron-Alkali Cation Pairs in Bulk Water. *J. Phys. Chem. B* **2006**, *110*, 607−615.
(37) Hofmeister, F. Zur Lehre von der Wirkung der Salze. *Arch. Pharmakol. Exp. Pathol.* **1888**, *25*, 1−30.
(38) Zhang, Y.; Cremer, P. S. Chemistry of Hofmeister Anions and Osmolytes. *Annu. Rev. Phys. Chem.* **2010**, *61*, 63−83.
(39) Han, P.; Bartels, D. Reevaluation of Arrhenius parameters for H + OH^- → $(e^-)_{aq}$ + H_2O and the enthalpy and entropy of hydrated electrons. *J. Phys. Chem.* **1990**, *94*, 7294−7299.
(40) Han, P.; Bartels, D. On the hydrated electron as a structure breaking ion. *J. Phys. Chem.* **1991**, *95*, 5367−5370.
(41) Collins, K. Charge density-dependent strength of hydration and biological structure. *Biophys. J.* **1997**, *72*, 65−76.
(42) Turi, L.; Borgis, D. Analytical Investigations of an Electron−Water Molecule Pseudopotential. II. Development of a New Pair Potential and Molecular Dynamics Simulations. *J. Chem. Phys.* **2002**, *117*, 6186−6195.
(43) Glover, W. J.; Larsen, R. E.; Schwartz, B. J. The Roles of Electronic Exchange and Correlation in Charge-Transfer-to-Solvent Dynamics: Many-Electron Nonadiabatic Mixed Quantum/Classical Simulations of Photoexcited Sodium Anions in the Condensed Phase. *J. Chem. Phys.* **2008**, *129*, 164505.
(44) Neupane, P.; Katiyar, A.; Bartels, D. M.; Thompson, W. H. Investigation of the Failure of Marcus Theory for Hydrated Electron Reactions. *J. Phys. Chem. Lett.* **2022**, *13*, 8971−8977.
(45) Duignan, T. T.; Parsons, D. F.; Ninham, B. W. A Continuum Solvent Model of the Partial Molar Volumes and Entropies of Ionic Solvation. *J. Phys. Chem. B* **2014**, *118*, 3122−3132.
(46) Phillips, J. C.; Kleinman, L. New Method for Calculating Wave Functions in Crystals and Molecules. *Phys. Rev.* **1959**, *116*, 287−294.
(47) Smallwood, C. J.; Larsen, R. E.; Glover, W. J.; Schwartz, B. J. A Computationally Efficient Exact Pseudopotential Method. I. Analytic Reformulation of the Phillips-Kleinman Theory. *J. Chem. Phys.* **2006**, *125*, No. 074102.
(48) Cohen, M. H.; Heine, V. Cancellation of Kinetic and Potential Energy in Atoms, Molecules, and Solids. *Phys. Rev.* **1961**, *122*, 1821−1826.
(49) Steinhauser, O. Reaction Field Simulation of Water. *Mol. Phys.* **1982**, *45*, 335−348.
(50) Feynman, R. P. Forces in Molecules. *Phys. Rev.* **1939**, *56*, 340−343.
(51) Verlet, L. Computer "Experiments" on Classical Fluids. I. Thermodynamical Properties of Lennard-Jones Molecules. *Phys. Rev.* **1967**, *159*, 98−103.
(52) Toukan, K.; Rahman, A. Molecular-Dynamics Study of Atomic Motions in Water. *Phys. Rev. B: Condens. Matter Mater. Phys.* **1985**, *31*, 2643−2648.
(53) Dang, L. X. Mechanism and Thermodynamics of Ion Selectivity in Aqueous Solutions of 18-Crown-6 Ether: A Molecular Dynamics Study. *J. Am. Chem. Soc.* **1995**, *117*, 6954−6960.
(54) Shibata, N.; Sato, H.; Sakaki, S.; Sugita, Y. Theoretical Study of Magnesium Fluoride in Aqueous Solution. *J. Phys. Chem. B* **2011**, *115*, 10553−10559.
(55) Allen, P.; Tildesley, D. J., Eds. *Computer simulation of liquids*; Clarendon Press: Oxford, 1987.
(56) Frenkel, D.; Smit, B., Eds. *Understanding Molecular Simulation*; Academic Press, Inc.: Orlando, FL, United States, 2001.
(57) Reiser, S.; Deublein, S.; Vrabec, J.; Hasse, H. Molecular Dispersion Energy Parameters for Alkali and Halide Ions in Aqueous Solution. *J. Chem. Phys.* **2014**, *140*, No. 044504.
(58) Joung, I. S.; Cheatham, T. E., III Determination of Alkali and Halide Monovalent Ion Parameters for Use in Explicitly Solvated Biomolecular Simulations. *J. Phys. Chem. B* **2008**, *112*, 9020−9041.
(59) Jensen, K. P.; Jorgensen, W. L. Halide, Ammonium, and Alkali Metal Ion Parameters for Modeling Aqueous Solutions. *J. Chem. Theory Comput* **2006**, *2*, 1499−1509.
(60) Chowdhuri, S.; Chandra, A. Dynamics of Halide Ion-Water Hydrogen Bonds in Aqueous Solutions: Dependence on Ion Size and Temperature. *J. Phys. Chem. B* **2006**, *110*, 9674−9680.
(61) Errougui, A.; Lahmidi, A.; Chtita, S.; Kouali, M. E.; Talbi, M. Hydration Structures and Dynamics of the Sodium Fluoride Aqueous Solutions at Various Temperatures: Molecular Dynamics Simulations. *J. Solution Chem.* **2023**, *52*, 176−186.
(62) Horinek, D.; Herz, A.; Vrbka, L.; Sedlmeier, F.; Mamatkulov, S. I.; Netz, R. R. Specific Ion Adsorption at the Air/Water Interface: The Role of Hydrophobic Solvation. *Chem. Phys. Lett.* **2009**, *479*, 173−183.
(63) Soper, A. K.; Weckström, K. Ion Solvation and Water Structure in Potassium Halide Aqueous Solutions. *Biophys. Chem.* **2006**, *124*, 180−191.
(64) Xantheas, S. S.; Dang, L. X. Critical Study of Fluoride-Water Interactions. *J. Phys. Chem.* **1996**, *100*, 3989−3995.
(65) Blazquez, S.; Conde, M. M.; Abascal, J. L. F.; Vega, C. The Madrid-2019 force field for electrolytes in water using TIP4P/2005 and scaled charges: Extension to the ions F^-, Br^-, I^-, Rb^+, and Cs^+. *J. Chem. Phys.* **2022**, *156*, No. 044505.
(66) Martyna, G. J.; Klein, M. L.; Tuckerman, M. Nose-Hoover chains: The canonical ensemble via continuous dynamics. *J. Chem. Phys.* **1992**, *97*, 2635−2643.
(67) Glover, W. J.; Casey, J. R.; Schwartz, B. J. Free Energies of Quantum Particles: The Coupled-Perturbed Quantum Umbrella Sampling Method. *J. Chem. Theory Comput.* **2014**, *10*, 4661−4671.
(68) Shirts, M. R.; Chodera, J. D. Statistically optimal analysis of samples from multiple equilibrium states. *J. Chem. Phys.* **2008**, *129*, 124105.
(69) Park, S. J.; Schwartz, B. J. Understanding the Temperature Dependence and Finite Size Effects in Ab Initio MD Simulations of the Hydrated Electron. *J. Chem. Theory Comput.* **2022**, *18*, 4973−4982.

https://doi.org/10.1021/acs.jpcb.4c04290
J. Phys. Chem. B 2024, 128, 8557−8566